CHAPTER 4

RESULTS AND DISCUSSIONS

4.0 AVAILABLE TIDAL DATA IN THE STRAITS OF MALACCA

Published tidal data in the form of co-range and co-tidal charts are available mainly in the southern part of the Straits of Malacca from Hydrographic Chart No 5084 (Real-Admiralty G.P.D.Hall, 1992), as reproduced in Figure 4.1. In addition, the amplitudes and phases for different tidal constituents i.e M2, S2, K1 and O1 are also available from published MONACO data (1990) and Admiralty Tides Tables and Tidal Streams Tables (1993, Vol. 2) for a number of tidal stations. Data available for fourteen tidal elevation stations along the coast of Peninsular Malaysia are chosen for the verification of the computed results. The locations of these tidal stations are shown in Figure 4.2 and their geographical and numerical scheme positions given in Table 4.1.

Three current meter stations are also available in the southern region. The locations of these stations are given in Figure 4.3 and Table 4.2. They are denoted as Station A, Station B and Station C. The observed current data from the Hydrographic Charts are given in terms of amplitude and direction of the tidal current during the spring and neap tides with reference to high water at Kuala Batu Pahat tidal station. The computed tidal currents for M2 and S2 components could be extracted to compare with this information. Comparison

between the observed and computed results of current speed for spring and neap tides would be discussed later.

Table 4.1 Name and location of tidal elevation stations chosen for verification of the computed results.

Tidal Elevation Stations	Latitude	Longitude	Coordinates in numerical mesh
1. Pulau Kafai	7.03°N	99.43°E	(32, 62)
2. Nth Cono Island	6.87°N	99.60°E	(35, 63)
3. Pulau Lela	6.73°N	99.70°E	(38, 62)
4. Bass Harbour	6.30°N	99.73°E	(44, 58)
5. Penang	5.42°N	100.35°E	(62, 54)
6. Penang	5.42°N	100.35°E	(62, 54)
7. Pulau Rimau	5.25°N	100.28°E	(63, 51)
8. Lumut Pier	4.23°N	100.62°E	(80, 43)
9. Port Swettenham	3.00°N	101.38°E	(103, 35)
10. One Fathom Bank	2.88°N	101.00°E	(100, 32)
11.Pintu Gedong	2.90°N	101.25°E	(103, 35)
12.Pulau Undam	2.05°N	102.33°E	(126, 38)
13.Muar	2.05°N	102.57°E	(129, 41)
14.Kuala Batu Pahat	1.80°N	102.88°E	(136, 41)

Table 4.2 Name and location of tidal current stations chosen for verification of the computed results.

Tidal Current Stations	Latitude	Longitude	Coordinates in numerical mesh
1. Station A, Off Raleigh Shoal	2.12°N	101.95°E	(121, 35)
2. Station B, Off Tanjung Segenting	1.63°N	102.73°E	(136, 38)
3. Station C, Off One Fathom Bank	2.67°N	101.17°E	(106, 31)

Figure 4.1: Co-range and co-tidal chart of the Straits of Malacca.

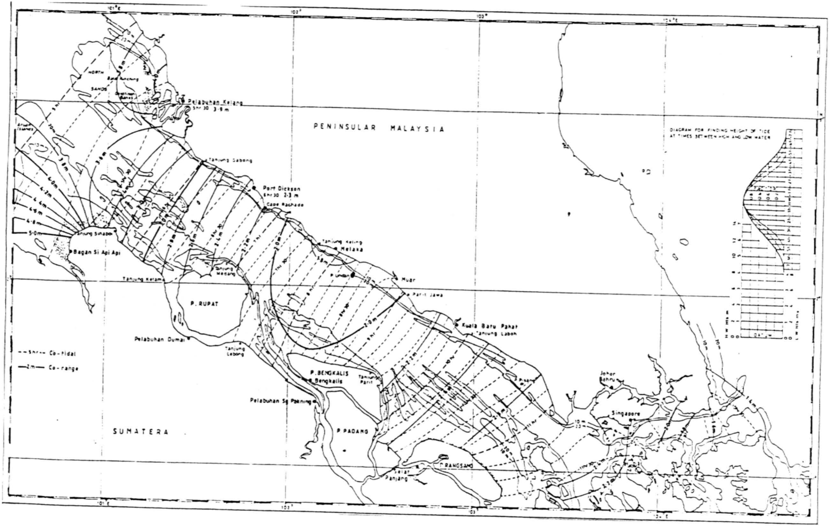

Figure 4.2 Location of selected tidal stations along the Straits of Malacca.

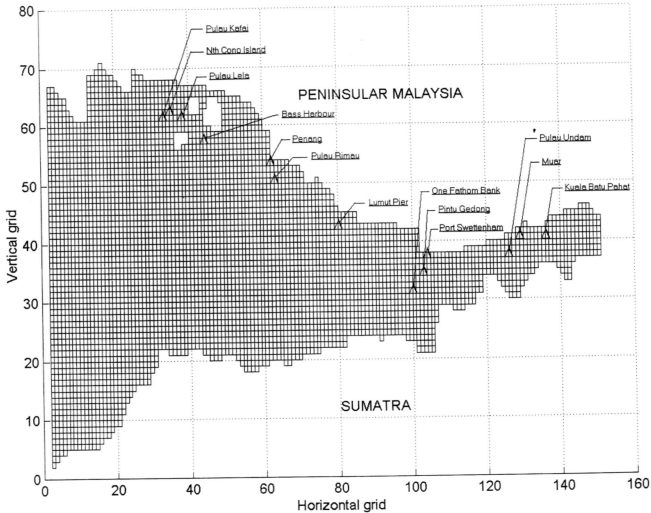

Figure 4.3 Location of current meter stations along the Straits of Malacca.

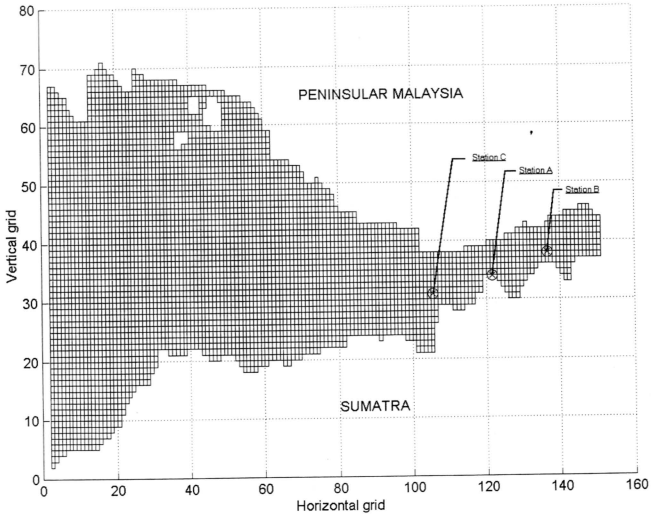

4.1 BEHAVIOUR OF THE NUMERICAL MODEL IN THE SPIN-UP PHASE

The transient numerical model is initiated from a calm sea state. With time marching, it goes through a period of self adjustment whereby the flow parameters ξ, P and Q are being updated continuously before settling down to oscillating patterns which are repeatable after the initial spin-up.

Several test runs were conducted to study the initial spin-up behaviour of the numerical model using typical input data on M2 and different time steps. The patterns of the predicted elevations for three stations representing the north (Pulau Kafai), middle (Pulau Rimau) and south (Kuala Batu Pahat) of the Straits of Malacca are shown in Figure 4.4 for time step of 30 seconds. The results show that the initial transients for the three tidal stations selected phased out and reached steady sinusoidal patterns within 24 hours or in about 2900 steps.

When a time step of 50 seconds which is marginally larger than the Courant-Friedrichs-Levy (CFL) criterion of 40 seconds was used, the results in Figure 4.5 show that only the predicted elevation at Kuala Batu Pahat tidal station seems to have achieved steady state within this period. For the other two stations, the main sinusoidal trends similar to the previous results were also formed after 24 hours but small wiggles riding on the sinusoidal curves persisted even after 48 hours. In other words, it would take longer time to phase out all the transients when larger time steps are used. However, when time step of 100 seconds was used in another test, the numerical scheme became very unstable whereby the predicted elevations were fluctuating indefinitely. This

shows that it is necessary to restrict the time step to the CFL condition to ensure good stability of the numerical scheme.

Figure 4.4 Predicted tidal elevations during the initial spin-up phase when time step =30 s .

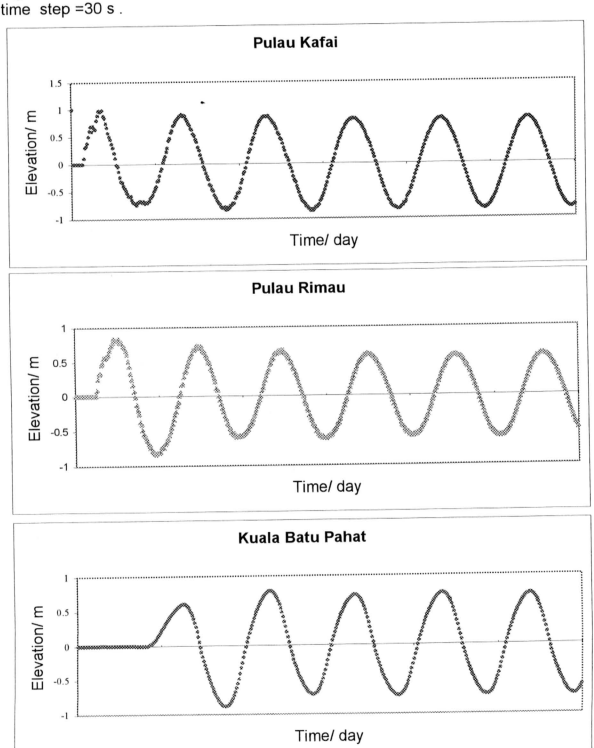

Figure 4.5 Predicted tidal elevations during the initial spin-up phase when time step =50 s.

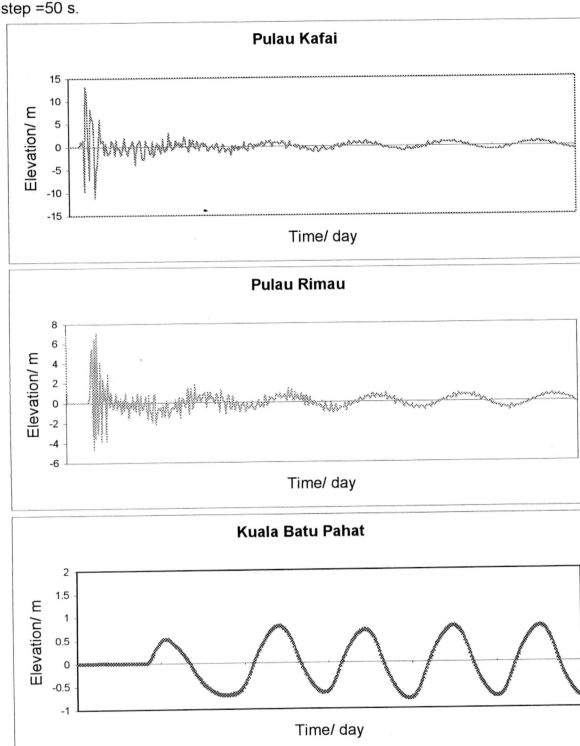

4.2 PARAMETRIC STUDY IN THE QUASI-STEADY OSCILLATING PHASE

For the purpose of testing the sensitivity of the model towards the changes in input parameters such as bottom friction coefficient and open boundary conditions which are poorly known, a series of tests is performed on the M2 component by varying these parameters systematically as summarized in Tables 4.3 to 4.6. It is assumed here that the trends obtained from M2 will also apply to other tidal constituents.

The first series of tests involves variation in the value of the drag coefficient C in the quadratic friction law (designated as D-1 to D-7). The second series involves a power law for C in the form of $C = C'h^n$ which was proposed by Guoy, 1989, in a slightly different way in order to best fit the model results. Several tests are carried out to investigate the degree of dependency of bottom friction on bathymetry depth.

The third series of tests with two different prescriptions of open boundary conditions are designated as O-1 and O-2. The tidal elevation prescribed on the open boundaries is given by

$$\xi = \xi_0 \cos(\omega t - \delta) \qquad (4.1)$$

where ξ_0 is the amplitude, ω is the angular frequency and δ is the phase difference in reference to Greenwich Standard Time(GST). The known values of harmonic constants of elevation and phase for M2 at both ends of Peninsular Malaysia and Sumatra are fitted linearly and sinusoidally to yield the intermediate values as shown in Figure 4.6 and Figure 4.7.

In the fourth series of tests, a correction factor is introduced into the prescription of the tidal elevations at the open boundaries, where $\xi = \xi_0 \cos(\omega t - \delta + \phi)$. A value of $\phi = 30^0$ is tested to investigate its influence on the computed amplitude and phase.

Table 4.3. Changing values of drag coefficient, C ($m^{1/2}s^{-1}$) in the quadratic friction law.

Test Series	D-1	D-2	D-3	D-4	D-5	D-6	D-7
Drag coefficient, C ($m^{1/2}s^{-1}$)	40	50	60	70	80	90	100

Table 4.4. Changing values of C' and n in the power law for drag coefficient, $C = C'h^n$

	C'	10	15	20	25	30	35	40	45	50
Test series	n=0.6	DA-1	DA-2	DA-3	DA-4	DA-5	DA-6	DA-7	DA-8	DA-9
	n=0.8	DB-1	DB-2	DB-3	DB-4	DB-5	DB-6	DB-7	DB-8	DB-9
	n=1.0	DC-1	DC-2	DC-3	DC-4	DC-5	DC-6	DC-7	DC-8	DC-9

Table 4.5. Varying tidal elevation curve fit at open boundaries. A drag coefficient of 65 $m^{1/2}s^{-1}$ is used.

Test series	Open boundary curve fit
O-1	Linear interpolation
O-2	Sinusoidal fitting

Table 4.6. Tidal phase corrections at open boundaries. Linear interpolation at the open boundaries and a drag coefficient of 65 $m^{1/2}s^{-1}$ is used.

Test series	O-1	OA-1
Phase correction	$\phi = 0^0$	$\phi = 30^0$

Figure 4.6 Different curve fit of tidal amplitudes for M2 at northern open boundary.

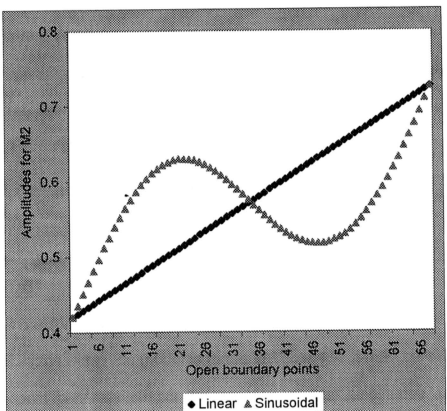

Figure 4.7: Different curve fit of amplitudes for M2 at southern open boundary points.

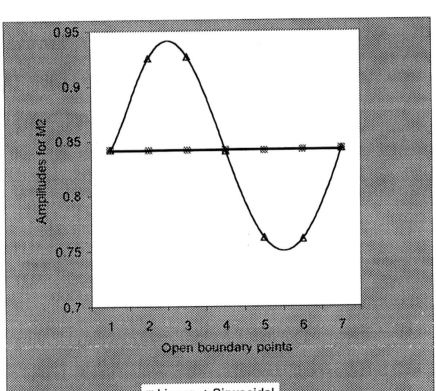

4.3 VARIATION OF DRAG COEFFICIENT IN THE QUADRATIC FRICTION LAW

In the first series of tests (D-1 to D-7), water depth is taken from the navigation map without adjustments and the open boundaries are linearly fitted. Values of drag coefficient tested range from 40 to 100. For each set, the root mean square error (RMSE) is computed from the predicted and published data at 14 tidal elevation stations as mentioned previously.

4.3.1 INFLUENCE OF DRAG COEFFICIENT ON M2 TIDAL AMPLITUDE

A comparison of observed and computed amplitudes for M2 component at the 14 locations within the model is made in Table 4.7. It may be seen that the model could generally predict the variation of tidal amplitudes at these stations and the predicted values are not too far away from the observed data. Also, the influence of the drag coefficient is noticeable from the changes in tabulated data as C is varied.

The RMSEs between the observed and computed amplitudes are shown in Table 4.7 and the trend plotted in Figure 4.8. An occurrence of minimum RMSE in the tidal amplitudes is clearly visible when C is between 60 and $70 m^{1/2} s^{-1}$. The achievable reduction in RMSE is nearly 200% between the minimum and maximum values. This shows that an 'optimum' drag coefficient that minimizes the overall difference between predicted and published values is achievable.

However, it is evident from Table 4.7 that for tidal stations at Pulau Kafai, North Cono Island, Pulau Lela and Bass Harbour, the predicted tidal amplitudes

best fit the observed values when smaller C values are used. Whereas, for tidal stations at Pulau Undam, Muar and Kuala Batu Pahat it seems larger C values exceeding $60m^{1/2}s^{-1}$ would better fit the observed elevation amplitude data. Incidentally, the two groups of tidal stations are located in the northern and southern part of the Straits respectively. It seems therefore different parameterizations of bottom friction may be required for different parts of the Straits due to its vastly different depth features.

It is also noted that reducing the bottom friction by way of increasing the drag coefficient produces amplification in the tidal amplitudes for the southern part, thus resulting in better predictions for those tidal stations that are very much under-predicted when smaller C values were used such as Port Swettenham, One Fathom Bank, Pintu Gedong, Pulau Undam, Muar and Kuala Batu Pahat. From an energy standpoint, reducing bottom friction also means allowing more energy to enter the Straits. This causes a surge in tidal elevations as the tidal waves enter the narrowing part of the Straits, thus resulting in a change from under-prediction to over-prediction of tidal amplitudes for tidal stations situated in the narrower part of the Straits such as Pintu Gedong, Pulau Undam and Muar.

Herein, we can conclude that the model prediction of amplitudes is sensitive to the change in drag coefficient which represents one of the major parameters often used for fine-tuning of model results.

Table 4.7: Comparison of observed and computed amplitudes for M2 component at 14 tidal stations for different values of C.

Tidal station	Observed	D-1	D-2	D-3	D-4	D-5	D-6	D-7
1. Pulau Kafai	0.814	0.808	0.815	0.819	0.821	0.821	0.820	0.816
2. Nth Cono Island	0.826	0.830	0.836	0.840	0.842	0.842	0.840	0.837
3. Pulau Lela	0.847	0.838	0.845	0.849	0.850	0.849	0.845	0.840
4. Bass Harbour	0.729	0.768	0.773	0.773	0.770	0.763	0.754	0.744
5. Penang	0.601	0.724	0.697	0.670	0.644	0.619	0.593	0.567
6. Penang	0.568	0.724	0.697	0.670	0.644	0.619	0.593	0.567
7. Pulau Rimau	0.530	0.672	0.640	0.608	0.578	0.550	0.521	0.493
8. Lumut Pier	0.747	0.706	0.716	0.713	0.707	0.701	0.695	0.692
9. Port Swettenham	1.362	0.957	1.086	1.167	1.216	1.244	1.257	1.260
10. One Fathom Bank	1.204	1.113	1.229	1.298	1.341	1.367	1.384	1.394
11. Pintu Gedong	1.216	0.991	1.120	1.202	1.253	1.282	1.298	1.305
12. Pulau Undam	0.661	0.372	0.489	0.596	0.693	0.779	0.854	0.919
13. Muar	0.634	0.404	0.534	0.656	0.767	0.865	0.952	1.027
14. Kuala Batu Pahat	0.774	0.411	0.547	0.676	0.792	0.896	0.986	1.064
RMSE:		0.199	0.125	0.078	0.073	0.098	0.130	0.162

Figure 4.8: Trend of root mean square error between observed and computed amplitudes for M2 component at 14 tidal stations for different values of C.

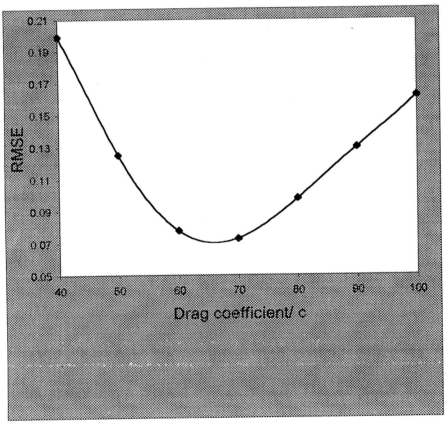

4.3.2 INFLUENCE OF DRAG COEFFICIENT ON M2 TIDAL PHASES.

A comparison of observed and computed phases in reference to GST for M2 component at the 14 locations within the model is made in Table 4.8. It may be seen that the model generally could not reproduce the tidal phases very well. The phases at Pulau Undam and Muar are over-predicted and those of the other stations are under-predicted. Generally, the results of the tests show that reducing the bottom friction by increasing the drag coefficient would cause the time for the occurrence of high water to be shifted forward.

Table 4.8: Comparison of observed and computed phases for M2 component at 14 tidal stations for different values of C.

Tidal station	Observed	D-1	D-2	D-3	D-4	D-5	D-6	D-7
1. Pulau Kafai	107.0	71.0	67.7	65.6	63.7	62.1	61.4	60.9
2. Nth Cono Island	108.8	73.3	69.6	67.0	64.9	63.3	61.9	60.2
3. Pulau Lela	112.1	77.7	73.7	70.5	67.9	66.1	64.4	63.0
4. Bass Harbour	129.7	90.8	85.9	82.1	79.1	76.5	74.7	73.3
5. Penang	154.3	120.1	113.6	108.5	104.5	101.7	99.4	97.5
6. Penang	152.8	120.1	113.6	108.5	104.5	101.7	99.4	97.5
7. Pulau Rimau	166.4	126.7	120.8	116.2	112.4	109.9	107.5	105.7
8. Lumut Pier	239.8	198.9	197.5	196.3	195.6	195.6	196.3	197.5
9. Port Swettenham	289.2	278.6	270.2	263.5	258.1	254.4	251.3	248.6
10. One Fathom Bank	284.0	248.6	244.4	240.9	238.1	236.0	234.1	232.5
11. Pintu Gedong	293.5	266.5	259.7	254.8	251.1	247.9	244.8	242.5
12. Pulau Undam	17.1	36.0	32.7	30.4	29.0	28.3	28.3	28.5
13. Muar	32.2	48.8	44.4	40.9	38.6	37.2	36.2	35.8
14. Kuala Batu Pahat	59.2	59.3	54.2	50.0	46.9	44.8	43.5	42.5
RMSE:		**31.0**	**34.9**	**38.1**	**40.7**	**42.7**	**44.3**	**45.6**

The RMSEs between the observed and computed phases for the 14 selected tidal stations are plotted in Figure 4.9. The trendline shows that the

RMSE is increasing monotonically and the computed phases at the tidal stations would depart further from the observed data with increasing drag coefficient except at Pulau Undam and Muar.

Thus, it can be concluded that the predicted phases could not be made to fit the observed data by fine-tuning the drag coefficient. The best value of C = 65 $m^{1/2}s^{-1}$ based on minimum RMSE for amplitude would result in a mean RMSE of 40^0 for phase.

Figure 4.9: Trend of root mean square error between observed and computed phases for M2 component at selected 14 tidal stations for different values of C.

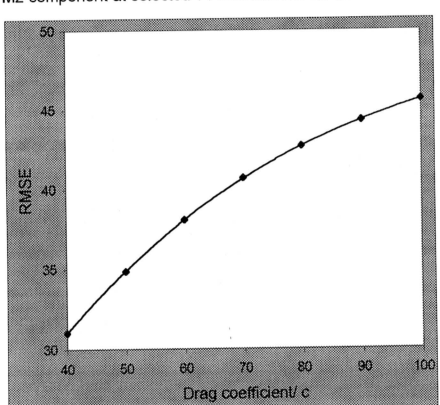

4.4 INVESTIGATION OF DEPTH DEPENDENCY OF DRAG COEFFICIENT IN A POWER LAW

In the second series of tests, the drag coefficient is in the form of a power law in terms of the bathymetric depth as described in section 4.2. The bathymetry depth and open boundary conditions used are the same as the first series of tests.

4.4.1 INFLUENCE OF COEFFICIENTS IN THE POWER LAW ON M2 TIDAL AMPLITUDE

Comparisons of computed amplitudes for M2 component at the 14 tidal stations within the model are shown in Tables 4.9 to 4.11. The predicted tidal amplitudes at these tidal stations are noticeably influenced by the coefficients in the power law namely C' and n. It is clearly visible in Figure 4.10 that a minimum RMSE occurs at a particular value of C' for each value of n. As n becomes larger, the corresponding C' that gives minimum RMSE will be smaller. It seems that the set of test where n=0.8 with a corresponding value of C' that lies between 20 to 25 gives the minimum RMSE amongst all the tests. Nevertheless, there is no significant reduction in RMSE for amplitude at these tidal stations compared to using the quadratic friction law.

Table 4.9: Comparison of computed amplitudes for M2 component at 14 tidal stations for n=0.6

Tidal station	Observed	DA-1	DA-2	DA-3	DA-4	DA-5	DA-6	DA-7	DA-8	DA-9
1. Pulau Kafai	0.814	0.803	0.806	0.812	0.816	0.818	0.817	0.815	0.812	0.810
2. Nth Cono Island	0.826	0.822	0.825	0.832	0.836	0.837	0.836	0.834	0.831	0.828
3. Pulau Lela	0.847	0.830	0.832	0.837	0.841	0.842	0840	0.836	0.832	0.828
4. Bass Harbour	0.729	0.754	0.753	0.758	0.759	0.754	0.747	0.739	0.731	0.723
5. Penang	0.601	0.740	0.691	0.648	0.618	0.592	0.568	0.545	0.524	0.505
6. Penang	0.568	0.740	0.691	0.648	0.618	0.592	0.568	0.545	0.524	0.505
7. Pulau Rimau	0.530	0.693	0.636	0.587	0.551	0.520	0.494	0.470	0.448	0.427
8. Lumut Pier	0.747	0.689	0.708	0.697	0.690	0.686	0.686	0.686	0.686	0.686
9. Port Swettenham	1.362	0.699	0.972	1.122	1.202	1.245	1.265	1.273	1.274	1.272
10. One Fathom Bank	1.204	1.000	1.217	1.316	1.365	1.389	1.402	1.409	1.412	1.413
11. Pintu Gedong	1.216	0.801	1.047	1.181	1.255	1.294	1.313	1.321	1.324	1.323
12. Pulau Undam	0.661	0.194	0.333	0.460	0.573	0.671	0.755	0.826	0.887	0.939
13. Muar	0.634	0.207	0.360	0.503	0.632	0.745	0.843	0.927	0.998	1.058
14. Kuala Batu Pahat	0.774	0.211	0.368	0.518	0.653	0.771	0.873	0.961	1.035	1.097
RMSE:		0.322	0.201	0.122	0.077	0.072	0.095	0.125	0.154	0.180

Table 4.10: Comparison of computed amplitudes for M2 component at 14 tidal stations for n=0.8

Tidal station	Observed	DB-1	DB-2	DB-3	DB-4	DB-5	DB-6	DB-7	DB-8	DB-9
1. Pulau Kafai	0.814	0.803	0.811	0.816	0.816	0.814	0.811	0.807	0.803	0.799
2. Nth Cono Island	0.826	0.821	0.829	0.835	0.835	0.832	0.828	0.824	0.820	0.817
3. Pulau Lela	0.847	0.828	0.834	0.839	0.838	0.833	0.828	0.822	0.817	0.812
4. Bass Harbour	0.729	0.748	0.753	0.753	0.744	0.735	0.725	0.715	0.707	0.699
5. Penang	0.601	0.688	0.630	0.594	0.563	0.534	0.508	0.485	0.464	0.445
6. Penang	0.568	0.688	0.630	0.594	0.563	0.534	0.508	0.485	0.464	0.445
7. Pulau Rimau	0.530	0.634	0.567	0.523	0.488	0.458	0.431	0.407	0.386	0.367
8. Lumut Pier	0.747	0.710	0.690	0.681	0.680	0.682	0.685	0.687	0.689	0.690
9. Port Swettenham	1.362	0.871	1.114	1.218	1.259	1.272	1.272	1.269	1.263	1.256
10. One Fathom Bank	1.204	1.212	1.340	1.386	1.404	1.412	1.415	1.416	1.415	1.414
11. Pintu Gedong	1.216	1.016	1.200	1.281	1.313	1.323	1.325	1.323	1.318	1.312
12. Pulau Undam	0.661	0.292	0.460	0.601	0.716	0.808	0.883	0.944	0.993	1.034
13. Muar	0.634	0.312	0.501	0.662	0.795	0.904	0.992	1.064	1.122	1.170
14. Kuala Batu Pahat	0.774	0.312	0.520	0.689	0.828	0.941	1.032	1.106	1.165	1.214
RMSE:		**0.233**	**0.123**	**0.073**	**0.085**	**0.120**	**0.155**	**0.185**	**0.211**	**0.232**

Table 4.11 Comparison of computed amplitudes for M2 component at 14 tidal stations for n=1.0

Tidal station	Observed	DC-1	DC-2	DC-3	DC-4	DC-5	DC-6	DC-7	DC-8	DC-9
1. Pulau Kafai	0.814	0.806	0.814	0.814	0.811	0.806	0.801	0.798	0.796	0.795
2. Nth Cono Island	0.826	0.824	0.831	0.832	0.828	0.823	0.818	0.814	0.811	0.809
3. Pulau Lela	0.847	0.828	0.834	0.833	0.827	0.820	0.814	0.808	0.804	0.801
4. Bass Harbour	0.729	0.747	0.747	0.737	0.724	0.712	0.702	0.693	0.686	0.680
5. Penang	0.601	0.627	0.580	0.543	0.508	0.477	0.452	0.431	0.414	0.398
6. Penang	0.568	0.627	0.580	0.543	0.508	0.477	0.452	0.431	0.414	0.398
7. Pulau Rimau	0.530	0.565	0.508	0.465	0.429	0.399	0.374	0.353	0.335	0.319
8. Lumut Pier	0.747	0.690	0.676	0.675	0.681	0.687	0.690	0.692	0.692	0.693
9. Port Swettenham	1.362	0.992	1.192	1.256	1.268	1.266	1.261	1.253	1.244	1.235
10. One Fathom Bank	1.204	1.337	1.394	1.411	1.416	1.417	1.417	1.415	1.413	1.410
11. Pintu Gedong	1.216	1.175	1.289	1.320	1.325	1.323	1.318	1.312	1.305	1.297
12. Pulau Undam	0.661	0.408	0.595	0.735	0.840	0.920	0.981	1.030	1.068	1.099
13. Muar	0.634	0.439	0.653	0.816	0.939	1.034	1.108	1.165	1.210	1.246
14. Kuala Batu Pahat	0.774	0.459	0.684	0.854	0.982	1.080	1.154	1.212	1.257	1.294
RMSE:		**0.162**	**0.080**	**0.094**	**0.137**	**0.176**	**0.207**	**0.233**	**0.254**	**0.270**

Figure 4.10: Trend of root mean square errors between observed and computed amplitudes for M2 component at selected 14 tidal stations for different values of n.

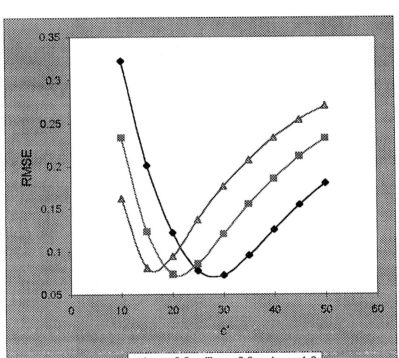

4.4.2 INFLUENCE OF COEFFICIENTS IN THE POWER LAW ON M2 PHASES

Comparisons of observed and computed phases in reference to GST for M2 component at the 14 tidal stations within the model are shown in Tables 4.12 to 4.14. It may be noticed that the model under-predicted the phases at most of the tidal stations except for Pulau Undam and Muar, where the phases were over-predicted.

Generally, the results of the tests show that increasing the value of n would cause the time for the occurrence of high water to be shifted forward, thus resulting in further under-predictions of phases in all the tidal stations except for Pulau Undam and Muar, where larger value of n will improve the prediction indeed. The RMSEs between the observed and computed phases for different values of n are plotted in Figure 4.11. The trendlines suggest that the RMSE is increasing monotonically and the computed phases at the tidal stations would depart further from the observed data with increasing value of n.

Thus, it can be concluded that the predicted phases could not be fine-tuned to fit the observed data by adjusting the power of depth dependency. The best value of C'=20 for n=0.8 based on the minimum RMSE for amplitude would result in a mean RMSE of about 43^0 for phase which is marginally larger than the case for quadratic friction law.

Table 4.12: Comparison of computed phases for M2 component at 14 tidal stations for n=0.6

Tidal station	Observed	DA-1	DA-2	DA-3	DA-4	DA-5	DA-6	DA-7	DA-8	DA-9
1. Pulau Kafai	107.0	73.3	68.2	64.9	62.6	61.6	61.4	61.4	56.5	56.3
2. Nth Cono Island	108.8	75.6	70.3	66.5	64.2	63.0	60.2	59.5	59.3	59.3
3. Pulau Lela	112.1	79.8	74.2	70.0	67.5	65.4	63.7	62.8	61.6	60.2
4. Bass Harbour	129.7	92.4	85.6	80.7	77.5	75.1	74.2	70.3	69.6	69.3
5. Penang	154.3	125.7	115.9	108.0	101.7	98.0	96.4	95.0	93.3	92.4
6. Penang	152.8	125.7	115.9	108.0	101.7	98.0	96.4	95.0	93.3	92.4
7. Pulau Rimau	166.4	131.1	122.5	115.0	110.8	107.3	105.0	103.1	102.7	102.7
8. Lumut Pier	239.8	200.1	198.9	198.2	198.2	198.0	198.0	198.0	197.7	202.2
9. Port Swettenham	289.2	303.6	286.1	272.8	263.2	257.2	253.0	250.2	247.6	245.1
10. One Fathom Bank	284.0	251.6	244.6	240.4	237.4	235.3	233.6	232.5	231.5	229.7
11. Pintu Gedong	293.5	274.7	263.9	255.3	249.9	246.9	244.1	241.3	239.7	238.3
12. Pulau Undam	17.1	42.1	35.5	31.1	28.8	27.6	27.6	28.1	28.8	29.5
13. Muar	32.2	60.7	51.4	44.4	40.4	38.1	37.2	36.5	36.5	36.5
14. Kuala Batu Pahat	59.2	68.4	57.9	50.4	46.0	43.5	42.1	41.4	41.1	41.1
RMSE:		**29.49**	**33.75**	**38.08**	**41.41**	**43.67**	**45.23**	**46.64**	**47.89**	**48.38**

Table 4.13: Comparison of computed phases for M2 component at 14 tidal stations for n=0.8

Tidal station	Observed	DB-1	DB-2	DB-3	DB-4	DB-5	DB-6	DB-7	DB-8	DB-9
1. Pulau Kafai	107.0	68.4	64.0	61.6	61.4	56.5	56.3	56.3	56.3	51.1
2 Nth Cono Island	108.8	70.5	65.6	63.3	59.8	59.3	59.3	59.1	59.1	59.1
3 Pulau Lela	112.1	74.2	69.1	65.8	63.5	62.8	60.5	59.3	59.1	59.1
4 Bass Harbour	129.7	85.6	79.1	75.6	74.4	69.8	69.6	69.3	69.1	69.1
5 Penang	154.3	116.2	106.4	98.5	95.0	93.3	92.2	91.9	91.9	86.6
6 Penang	152.8	116.2	106.4	98.5	95.0	93.3	92.2	91.9	91.9	86.6
7. Pulau Rimau	166.4	122.5	113.4	108.5	104.0	102.7	102.4	96.8	96.8	96.8
8. Lumut Pier	239.8	198.9	198.2	198.4	198.4	198.0	202.2	202.4	202.6	202.6
9. Port Swettenham	289.2	298.4	276.5	262.8	254.8	250.4	246.9	244.1	242.0	240.6
10. One Fathom Bank	284.0	244.1	239.0	235.7	233.4	232.2	231.3	228.0	227.6	227.1
11. Pintu Gedong	293.5	265.1	153.4	246.7	244.1	240.6	238.3	236.9	235.7	234.3
12. Pulau Undam	17.1	36.7	30.4	27.8	27.4	27.6	28.5	29.9	31.1	31.8
13. Muar	32.2	55.6	45.1	39.7	37.6	36.9	36.9	37.2	37.4	37.9
14. Kuala Batu Pahat	59.2	59.8	48.8	43.7	41.1	40.4	40.7	40.9	41.1	41.4
RMSE:		**33.96**	**39.06**	**43.05**	**45.52**	**47.47**	**48.15**	**49.43**	**49.75**	**51.37**

Table 4.14: Comparison of computed phases for M2 component at 14 tidal stations for n=1.0

Tidal station	Observed	DC-1	DC-2	DC-3	DC-4	DC-5	DC-6	DC-7	DC-8	DC-9
1. Pulau Kafai	107.0	64.0	61.6	56.5	56.3	56.3	56.3	51.1	51.1	51.1
2. Nth Cono Island	108.8	65.8	63.3	59.5	59.3	59.1	59.1	59.1	58.8	58.8
3. Pulau Lela	112.1	69.1	65.1	63.0	59.8	59.1	58.8	59.1	59.3	59.5
4. Bass Harbour	129.7	78.9	74.9	70.0	69.6	69.3	69.1	69.1	68.9	68.9
5. Penang	154.3	107.3	97.1	92.4	91.7	87.5	86.8	86.3	86.3	86.3
6. Penang	152.8	107.3	97.1	92.4	91.7	87.5	86.8	86.3	86.3	86.3
7. Pulau Rimau	166.4	114.5	107.8	102.4	102.2	96.8	96.8	96.6	96.6	96.6
8. Lumut Pier	239.8	198.2	198.4	201.2	202.2	202.4	202.6	202.6	202.9	207.5
9. Port Swettenham	289.2	291.7	267.9	255.3	249.0	245.1	242.3	240.6	239.5	238.3
10. One Fathom Bank	284.0	238.8	234.6	232.5	231.5	227.8	227.3	226.9	226.9	226.6
11. Pintu Gedong	293.5	254.6	245.3	242.5	238.1	236.2	234.8	232.9	232.7	232.0
12. Pulau Undam	17.1	31.1	27.4	27.4	27.8	29.5	31.3	32.5	33.4	34.6
13. Muar	32.2	49.5	40.9	37.9	37.4	37.6	37.9	38.3	38.8	39.3
14. Kuala Batu Pahat	59.2	49.7	42.3	39.7	40.0	40.4	40.9	41.4	41.8	42.3
RMSE:		**38.71**	**43.56**	**47.00**	**48.20**	**50.28**	**50.79**	**51.59**	**51.70**	**51.64**

Figure 4.11: Trend of root mean square errors between observed and computed phases for M2 component at selected 14 tidal stations for different values of n.

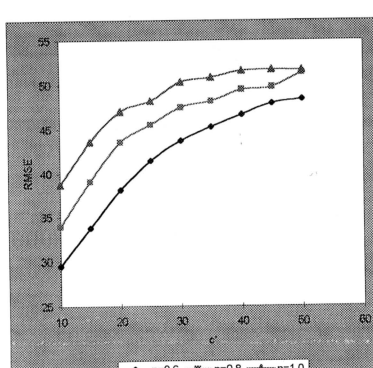

4.5 INVESTIGATION OF DIFFERENT CURVE FITTING OF ELEVATION AT THE OPEN BOUNDARIES

In the third series of tests, the bottom friction is in the quadratic form and the drag coefficient used is 65 $m^{1/2}s^{-1}$. Between the linear and sinusoidal curve fits, the former is mathematically exact since there are only two known points across the open boundaries. For the latter, there are in theory many sine curves which will pass through two points. By specifying the frequency to be equal to the tidal component frequency, there is a unique sine curve which satisfies the two points.

4.5.1 INFLUENCE OF DIFFERENT FITTING OF ELEVATION AT THE OPEN BOUNDARIES ON TIDAL AMPLITUDES

The comparison of observed and computed M2 tidal amplitudes using the linear and sinusoidal curve fitting of open boundary condition is summarized in Table 4.15. It may be seen that by changing the prescription of tidal elevations at open boundaries, the effect on the computed amplitudes is not very significant. In fact, the RMSE becomes larger with sinusoidal curve fitting, though at certain stations the computed values were brought closer to the observed values with this curve fit.

4.5.2 INFLUENCE OF DIFFERENT FITTING OF ELEVATION AT THE OPEN BOUNDARIES ON TIDAL PHASES

The comparison of observed and predicted M2 tidal phases is shown in Table 4.16. The overall prediction of the phases improves slightly with sinusoidal

curve fitting of the boundary values. The phases were brought marginally closer to the observations for most of the tidal stations.

Table 4.15: Comparison of observed and computed amplitudes for M2 component at 14 tidal stations. Quadratic law is adopted and drag coefficient of 65 $m^{1/2}s^{-1}$ is used.

Tidal station	Observed	O-1	O-2
1. Pulau Kafai	0.814	0.820	0.816
2. Nth Cono Island	0.826	0.842	0.839
3. Pulau Lela	0.847	0.850	0.851
4. Bass Harbour	0.729	0.772	0.788
5. Penang	0.601	0.657	0.680
6. Penang	0.568	0.657	0.680
7. Pulau Rimau	0.530	0.593	0.615
8. Lumut Pier	0.747	0.710	0.734
9. Port Swettenham	1.362	1.195	1.227
10. One Fathom Bank	1.204	1.322	1.360
11. Pintu Gedong	1.216	1.231	1.264
12. Pulau undam	0.661	0.646	0.656
13. Muar	0.634	0.713	0.724
14. Kuala Batu Pahat	0.774	0.735	0.746
RMSE:		**0.070**	**0.077**

Table 4.16: Comparison of observed and computed phases for M2 component at 14 tidal stations. Quadratic law is adopted and drag coefficient of 65 $m^{1/2}s^{-1}$ is used.

Tidal station	Observed	O-1	O-2
1. Pulau Kafai	107.0	64.4	66.1
2. Nth Cono Island	108.8	65.8	67.5
3. Pulau Lela	112.1	69.1	70.7
4. Bass Harbour	129.7	80.5	81.2
5. Penang	154.3	106.4	106.6
6. Penang	152.8	106.4	106.6
7. Pulau Rimau	166.4	114.3	114.3
8. Lumut Pier	239.8	195.9	195.4
9. Port Swettenham	289.2	260.7	260.4
10. One Fathom Bank	284.0	239.5	239.0
11. Pintu Gedong	293.5	252.7	252.5
12. Pulau undam	17.1	29.7	29.0
13. Muar	32.2	39.7	39.3
14. Kuala Batu Pahat	59.2	48.3	47.9
RMSE:		**39.47**	**39.09**

4.6 INVESTIGATION OF PHASE CORRECTION IN THE PRESCRIPTION OF TIDAL ELEVATION AT THE OPEN BOUNDARIES

In the fourth series of tests, the bottom friction is in the quadratic form and the drag coefficient used is 65 $m^{1/2}s^{-1}$. A correction factor is introduced into the prescription of tidal elevation phase at the open boundaries.

4.6.1 INFLUENCE OF PHASE CORRECTION AT THE OPEN BOUNDARIES ON TIDAL AMPLITUDES

The comparison of observed and computed M2 tidal amplitudes with phase correction is summarized in Table 4.17. It seems changing the prescription of tidal elevations at open boundaries by introducing a correction factor to the phase has rather significant but worse effect on the computed amplitudes. In fact, the amplitudes at all the tidal stations were significantly reduced, which actually caused the predicted amplitude to deviate further from the observed one, thus an increase in the RMSE.

4.6.2 INFLUENCE OF PHASE CORRECTION AT THE OPEN BOUNDARIES ON TIDAL PHASES

The comparison of observed and predicted M2 tidal phases is shown in Table 4.18. The phase was shifted backward by introducing the correction factor and the overall prediction of the phases improves significantly with this adjustment. The computed phase for most of the tidal stations was brought closer to the

observed one except for tidal stations at Pulau Undam, Muar and Kuala Batu Pahat. The RMSE is reduced by about 47 % from 39.47^0 to 20.86^0.

Table 4.17: Comparison of observed and computed amplitudes for M2 component at 14 tidal stations with and without phase correction at the open boundaries. Quadratic law , linear curve fit at open boundaries and drag coefficient of $65m^{1/2}s^{-1}$ are used.

Tidal station	Observed	O-1	OA-1
1. Pulau Kafai	0.814	0.820	0.607
2. Nth Cono Island	0.826	0.842	0.623
3. Pulau Lela	0.847	0.850	0.629
4. Bass Harbour	0.729	0.772	0.571
5. Penang	0.601	0.657	0.472
6. Penang	0.568	0.657	0.472
7. Pulau Rimau	0.530	0.593	0.421
8. Lumut Pier	0.747	0.710	0.526
9. Port Swettenham	1.362	1.195	0.922
10. One Fathom Bank	1.204	1.322	1.014
11. Pintu Gedong	1.216	1.231	0.950
12. Pulau Undam	0.661	0.646	0.552
13. Muar	0.634	0.713	0.613
14. Kuala Batu Pahat	0.774	0.735	0.634
RMSE:		**0.070**	**0.203**

Table 4.18: Comparisons of observed and computed phases for M2 component at 14 tidal stations with and without phase correction at the open boundaries. Quadratic law, linear curve fit at the open boundaries and drag coefficient of 65 $m^{1/2}s^{-1}$ are used.

Tidal station	Observed	O-1	OA-1
1. Pulau Kafai	107.0	64.4	97.1
2. Nth Cono Island	108.8	65.8	98.0
3. Pulau Lela	112.1	69.1	101.0
4. Bass Harbour	129.7	80.5	111.7
5. Penang	154.3	106.4	136.9
6. Penang	152.8	106.4	136.9
7. Pulau Rimau	166.4	114.3	145.1
8. Lumut Pier	239.8	195.9	229.4
9. Port Swettenham	289.2	260.7	290.0
10. One Fathom Bank	284.0	239.5	270.9
11. Pintu Gedong	293.5	252.7	283.3
12. Pulau undam	17.1	29.7	62.6
13. Muar	32.2	39.7	71.7
14. Kuala Batu Pahat	59.2	48.3	79.6
RMSE:		**39.47**	**20.86**

4.7 COMPARISON BETWEEN COMPUTED RESULTS AND PUBLISHED DATA

From the results obtained in the parametric investigations in the previous sections, it may be seen that the 'best' prediction for the M2 tidal amplitudes and phases is obtained using the quadratic friction law with C = $65m^{1/2}s^{-1}$ and linear curve fit at the open boundaries. Using these conditions, the two-dimensional model is run to compute for M2, S2, K1 and O1 components and compare with observed amplitudes and phases at fourteen locations where tidal gauge data are available. The co-range and co-tidal results for all the four components will be plotted to show the spatial distribution of the tides in the Straits.

Since current data is available in terms of speed and direction of spring and neap tides at three current meter stations as mentioned in section 4.0 (Hydrographic Chart No 3946 and 3947), therefore the computed current speeds for M2 and S2 components and tidal stream directions at these three current meter stations will be combined vectorially for comparisons with the observed data. The tidal current flow patterns in the Straits when high water occurs at Kuala Batu Pahat will be shown.

4.7.1 TIDAL AMPLITUDE AND PHASE COMPARISON FOR M2 COMPONENT

The comparison between the computed and observed amplitudes of M2 component at the selected tidal stations is shown in Table 4.19 and Figure 4.12. It may be observed that the predicted amplitudes match the observed data very well

at most of the stations. The RMSE for the predicted amplitudes is 0.072 m with a maximum error of 0.167m at Port Swettenham.

The comparison between the computed and observed phases of M2 component is shown in Table 4.20 and Figure 4.13. The computed phases tend to be smaller than the observed data except at Port Swettenham, Pulau Undam and Muar. Overall, the RMSE for the phase is 7.84^0 with a maximum error of $+12.6^0$ at Pulau Undam.

Figures 4.14 and 4.15 show the computed M2 co-range and co-tidal charts in the Straits respectively. The co-range chart shows that the maximum M2 amplitude occurs off Port Klang near the mouth of the narrowest part of the Straits. This seems to agree very well with the results of Guoy, 1989, Hadi,1992, Lee, 1994 and Hydrograhic Chart No 5084 .

Table 4.19: Comparison of computed and observed amplitudes for M2 component.

Tidal station	Observed	Computed	Difference
1. Pulau Kafai	0.814	0.820	+0.006
2. Nth Cono Island	0.826	0.842	+0.016
3. Pulau Lela	0.847	0.850	+0.003
4. Bass Harbour	0.729	0.772	+0.043
5. Penang	0.601	0.657	+0.056
6. Penang	0.568	0.657	-0.011
7. Pulau Rimau	0.530	0.593	+0.063
8. Lumut Pier	0.747	0.710	-0.037
9. Port Swettenham	1.362	1.195	-0.167
10. One Fathom Bank	1.204	1.322	+0.118
11. Pintu Gedong	1.216	1.231	+0.015
12. Pulau Undam	0.661	0.646	-0.015
13. Muar	0.634	0.713	+0.079
14. Kuala Batu Pahat	0.774	0.735	-0.039
RMSE:			**0.070**

Figure 4.12: Comparison of computed and observed amplitudes for M2 component.

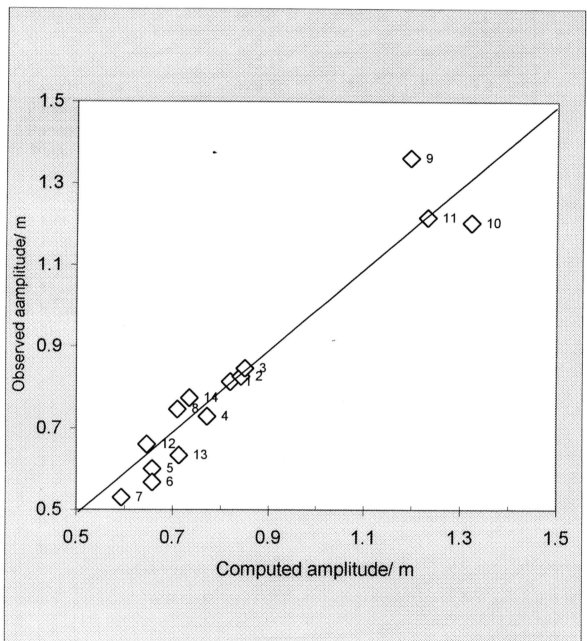

Table 4.20 Comparison of computed and observed phases for M2 component

Tidal station	Observed	Computed	Difference
1. Pulau Kafai	107.0	104.4	-2.6
2 Nth Cono Island	108.8	105.8	-3.0
3 Pulau Lela	112.1	109.1	-3.0
4 Bass Harbour	129.7	120.5	-9.2
5 Penang	154.3	146.4	-7.9
6 Penang	152.8	146.4	-6.4
7. Pulau Rimau	166.4	154.3	-12.1
8. Lumut Pier	239.8	235.9	-3.9
9. Port Swettenham	289.2	300.7	+11.5
10. One Fathom Bank	284.0	279.5	-4.5
11. Pintu Gedong	293.5	292.7	-0.8
12. Pulau Undam	17.1(377.1)	29.7(389.7)	+12.6
13. Muar	32.2(392.2)	39.7(399.7)	+7.5
14. Kuala Batu Pahat	59.2(419.2)	48.3(408.3)	-10.9
RMSE:			**7.84**

Figure 4.13: Comparison of computed and observed phases for M2 component.

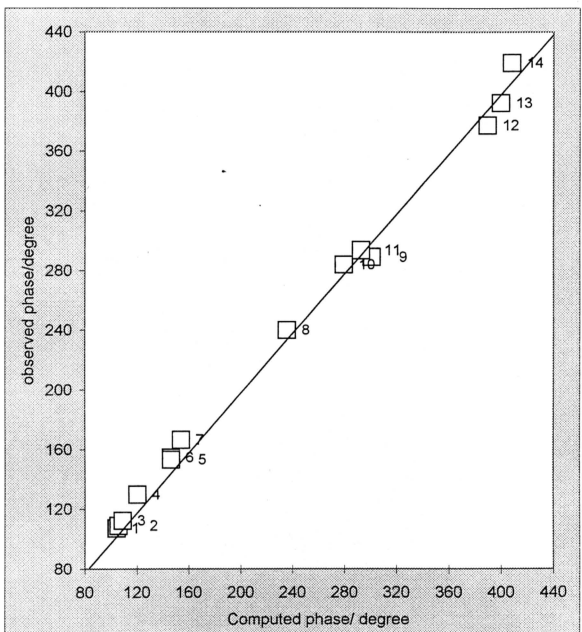

Figure 4.14: Computed co-range chart for M2 component in reference to Greenwich Standard Time.

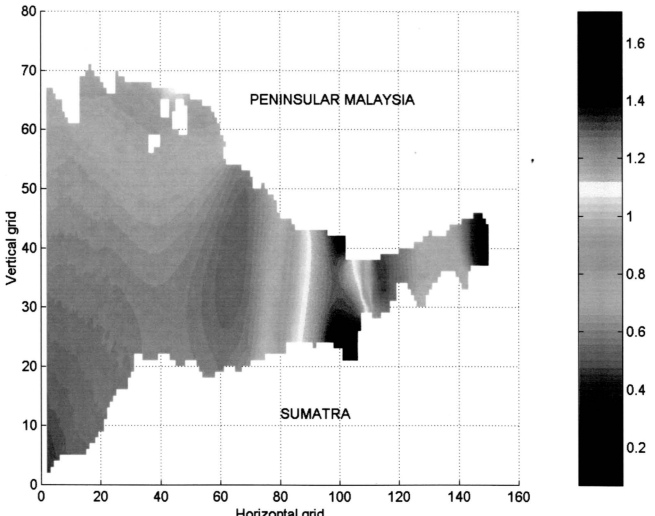

Figure 4.15: Computed co-tidal chart for M2 component in reference to Greenwich Standard Time.

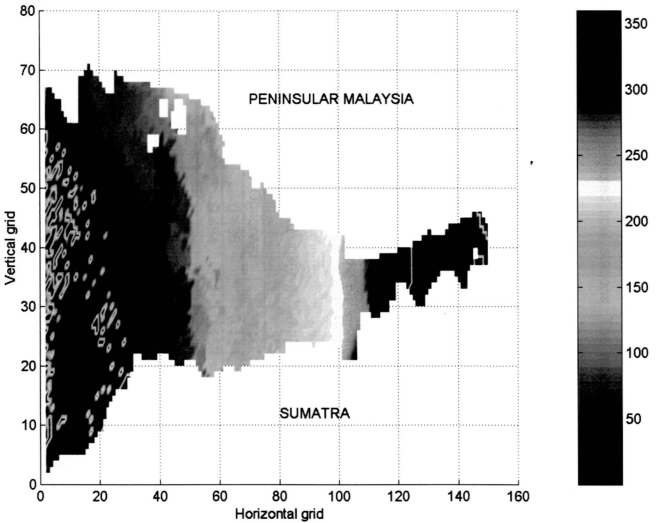

4.7.2 TIDAL AMPLITUDE AND PHASE COMPARISON FOR S2 COMPONENT

Table 4.21 and Figure 4.16 show the comparison of the computed and observed amplitude at 14 selected tidal stations. The model underpredicts the amplitude at all the tidal stations, with a RMSE of 0.277 m.

The model is able to predict the S2 phases to a satisfying degree of accuracy as shown in Table 4.22 and Figure 4.17 in which the computed phases yield a RMSE of 20.38^0.

Figures 4.18 and 4.19 show the computed S2 co-range and co-tidal charts in the Straits respectively. The co-range chart shows that maximum S2 amplitude occurs near the same place as in M2 due to the constriction further down.

Table 4.21 Comparison of computed and observed amplitudes for S2 component

Tidal station	Observed	Computed	Difference
1. Pulau Kafai	0.436	0.154	-0.282
2. Nth Cono Island	0.454	0.159	-0.295
3. Pulau Lela	0.494	0.160	-0.334
4. Bass Harbour	0.410	0.143	-0.267
5. Penang	0.347	0.100	-0.247
6. Penang	0.334	0.100	-0.234
7. Pulau Rimau	0.290	0.083	-0.207
8. Lumut Pier	0.363	0.113	-0.250
9. Port Swettenham	0.680	0.239	-0.441
10. One Fathom Bank	0.637	0.263	-0.374
11. Pintu Gedong	0.604	0.248	-0.356
12. Pulau Undam	0.323	0.197	-0.126
13. Muar	0.299	0.225	-0.074
14. Kuala Batu Pahat	0.372	0.236	-0.136
RMSE:			**0.277**

Figure 4.16: Comparison of computed and observed amplitudes for S2 component.

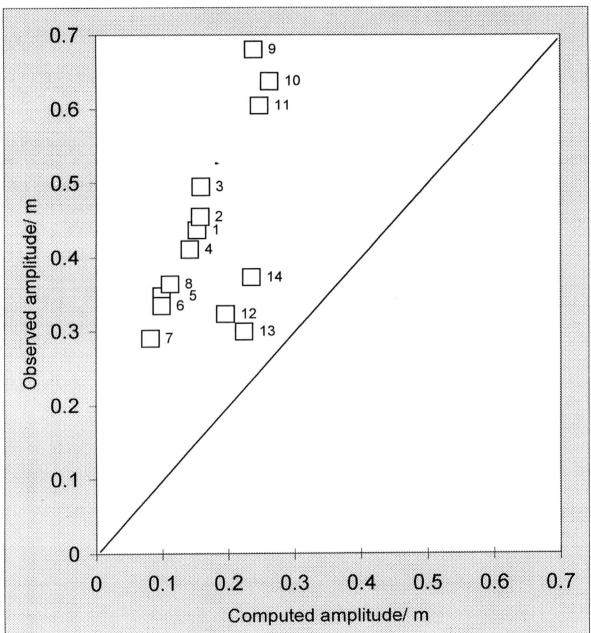

Table 4.22 Comparison of computed and observed phases for S2 component

Tidal station	Observed	Computed	Difference
1. Pulau Kafai	143.0	138.7	-4.3
2 Nth Cono Island	147.8	138.7	-9.1
3 Pulau Lela	150.0	138.5	-11.5
4 Bass Harbour	165.9	143.0	-22.9
5 Penang	190.3	165.2	-25.1
6 Penang	194.0	165.2	-28.8
7. Pulau Rimau	199.4	172.5	-26.9
8. Lumut Pier	273.8	267.2	-6.6
9. Port Swettenham	331.2	304.8	-26.4
10. One Fathom Bank	326.0	298.5	-27.5
11. Pintu Gedong	334.5	301.3	-33.2
12. Pulau Undam	61.0(421.0)	62.5(422.5)	+1.5
13. Muar	74.0(434.0)	58.5(418.5)	-15.5
14. Kuala Batu Pahat	101.2(461.2)	107.0(467.0)	+5.8
RMSE:			**20.38**

Figure 4.17: Comparison of computed and observed phases for S2 component.

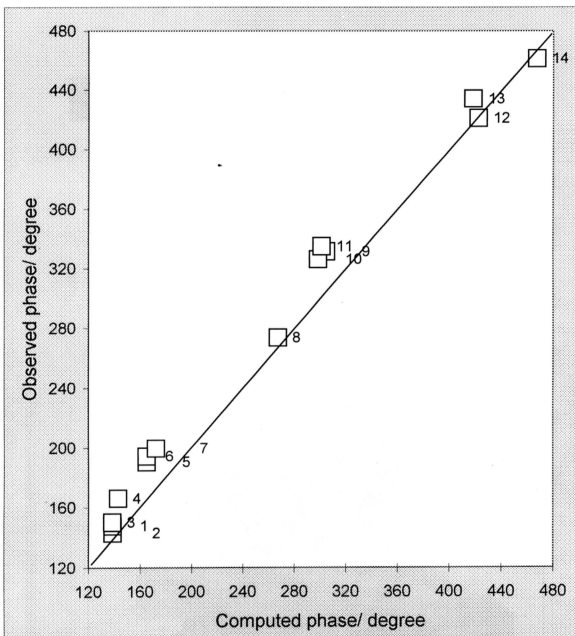

Figure 4.18: Computed co-range chart for S2 component in reference to Greenwich Standard Time.

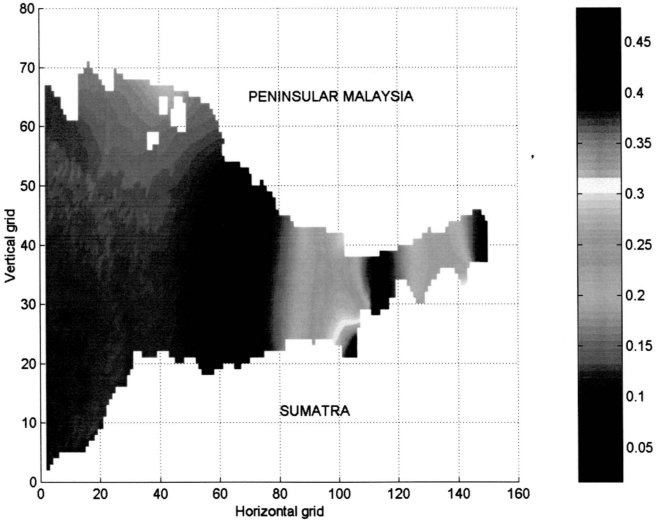

Figure 4.19: Computed co-tidal chart for S2 component in reference to Greenwich Standard Time.

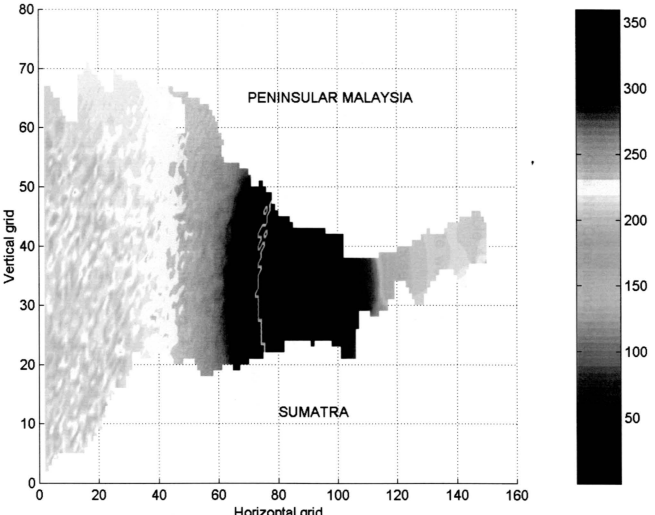

4.7.3 TIDAL AMPLITUDE AND PHASE COMPARISON FOR K1 COMPONENT

The comparison of computed and observed K1 amplitudes at selected tidal stations is shown in Table 4.23 and Figure 4.20. The model seems to predict well for the tidal stations at Pulau Kafai, Nth Cono Island, Pulau Lela and Bass Harbour which are situated in the northern part of the Straits but overpredict for tidal stations located to the south of Lumut Pier. The comparison between the computed and observed K1 phases shown in Table 4.24 and Figure 4.21 indicates that the model is able to predict the phases quite well. The phases at most of the tidal stations are slightly overpredicted while those at Pulau Kafai, Nth Cono island, Pulau lela and bass Harbour are underpredicted.

Overall, the computed co-range chart for K1 component plotted in Figure 4.22 shows that larger K1 amplitude occurs in the southern part of the Straits which suggests a strong influence of the diurnal component here as reported in previous works. The co-tidal chart in Figure 4.23 shows a progressive phase shift towards the southern part which is consistent with those obtained for the M2 and S2 components.

Table 4.23 Comparison of computed and observed amplitudes for K1 component

Tidal station	Observed	Computed	Difference
1. Pulau Kafai	0.149	0.144	-0.005
2. Nth Cono Island	0.162	0.148	-0.014
3. Pulau Lela	0.189	0.156	-0.033
4. Bass Harbour	0.178	0.179	+0.001
5. Penang	0.174	0.245	+0.071
6. Penang	0.177	0.245	+0.068
7. Pulau Rimau	0.216	0.256	+0.040
8. Lumut Pier	0.204	0.368	+0.164
9. Port Swettenham	0.184	0.491	+0.307
10. One Fathom Bank	0.140	0.482	+0.342
11. Pintu Gedong	0.128	0.489	+0.361
12. Pulau Undam	0.119	0.495	+0.376
13. Muar	0.137	0.472	+0.335
14. Kuala Batu Pahat	0.152	0.405	+0.253
RMSE:			**0.223**

Figure 4.20: Comparison of computed and observed amplitudes for K1 component

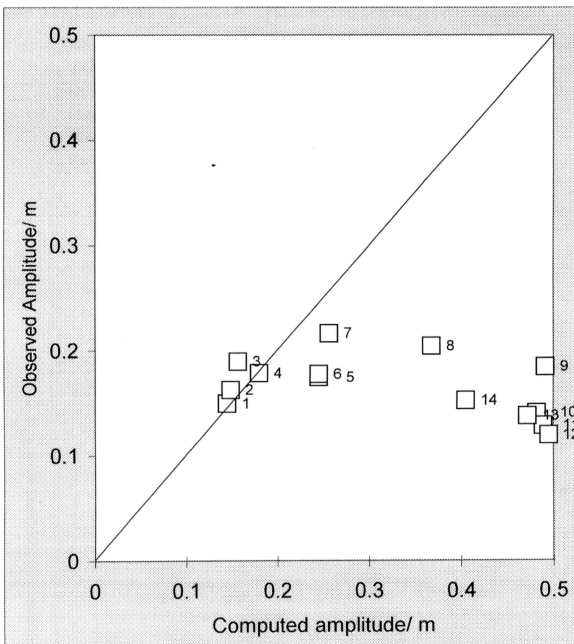

Table 4.24 Comparison of computed and observed phases for K1 component

Tidal station	Observed	Computed	Difference
1. Pulau Kafai	226.5	220.5	-6.0
2 Nth Cono Island	232.4	222.0	-10.4
3 Pulau Lela	223.7	223.1	-0.6
4 Bass Harbour	235.7	233.3	-2.4
5 Penang	239.7	245.9	+6.2
6 Penang	239.4	245.9	+6.5
7. Pulau Rimau	240.7	249.0	+8.3
8. Lumut Pier	240.4	263.5	+23.1
9. Port Swettenham	269.6	287.4	+17.8
10. One Fathom Bank	273	275.9	+2.9
11. Pintu Gedong	274.8	284.1	+9.3
12. Pulau Undam	49.8(409.8)	77.9(437.9)	+28.1
13. Muar	43.7(403.7)	70.0(437.7)	+34.0
14. Kuala Batu Pahat	48.1(408.1)	74.8(434.8)	+26.7
RMSE:			**16.70**

Figure 4.21: Comparison of computed and observed phases for K1 component.

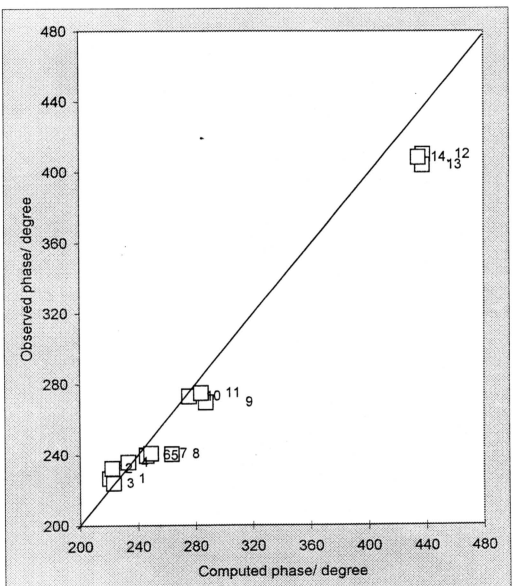

Figure 4.22: Computed co-range chart for K1 component in reference to Greenwich Standard Time.

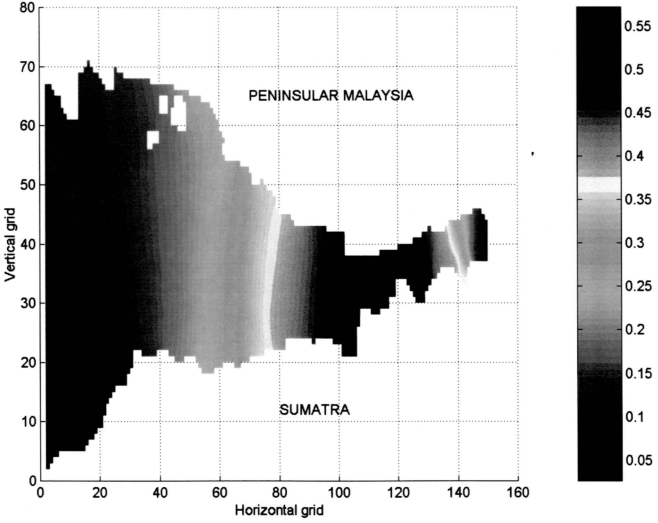

Figure 4.23: Computed co-tidal chart for K1 component in reference to Greenwich Standard Time.

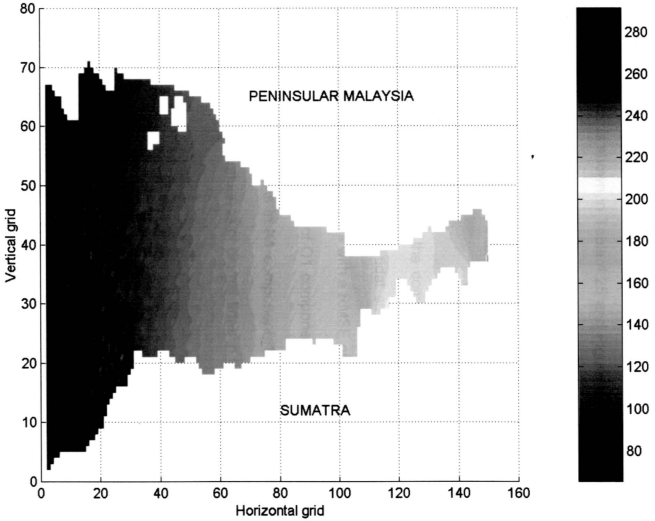

4.7.4 TIDAL AMPLITUDE AND PHASE COMPARISON FOR O1 COMPONENT

The comparison of computed and observed amplitudes for O1 component at the selected tidal stations is shown in Table 4.25 and Figure 4.24. The prediction accuracy of the model is somewhat mixed with amplitudes of some northern and southern tidal stations matching very well with the observed values but some match poorly. The amplitudes at seven intermediate tidal stations from Penang to Pulau Gedong are poorly predicted.

Table 4.26 and Figure 4.25 show the comparison between the computed and observed O1 phases at the selected tidal stations. The computed phases compare poorly against the observed ones with a RMSE of about 49.65^0.

The co-range and co-tidal charts of O1 component for the entire Straits are shown in Figures 4.26 and 4.27. As in K1 component, the model is qualitatively correct in revealing the strong influence of diurnal tides in the southern part of the Straits.

Table 4.25 Comparison of computed and observed amplitudes for O1component

Tidal station	Observed	Computed	Difference
1. Pulau Kafai	0.040	0.067	+0.027
2. Nth Cono Island	0.058	0.069	+0.011
3. Pulau Lela	0.052	0.072	+0.020
4. Bass Harbour	0.051	0.085	+0.034
5. Penang	0.042	0.117	+0.075
6. Penang	0.059	0.117	+0.058
7. Pulau Rimau	0.043	0.123	+0.080
8. Lumut Pier	0.052	0.171	+0.119
9. Port Swettenham	0.034	0.235	+0.201
10. One Fathom Bank	0.040	0.223	+0.183
11. Pintu Gedong	0.052	0.232	+0.180
12. Pulau Undam	0.201	0.230	+0.029
13. Muar	0.229	0.217	-0.012
14. Kuala Batu Pahat	0.256	0.183	-0.073
RMSE:			**0.102**

Figure 4.24: Comparison of computed and observed amplitudes for O1component

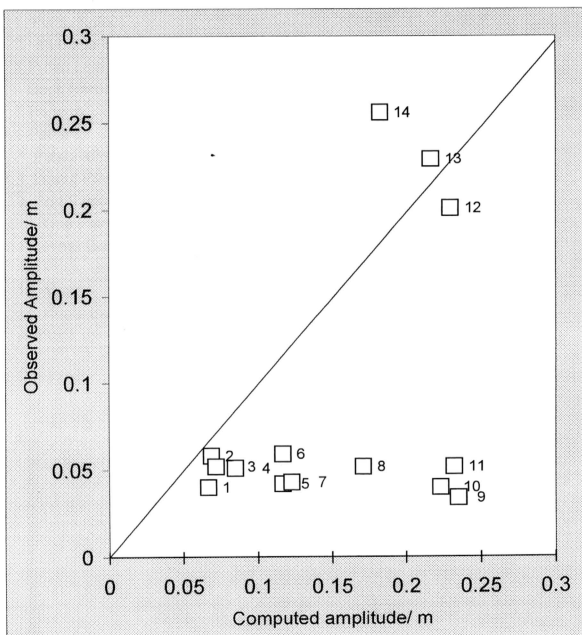

Table 4.26 Comparison of computed and observed phases for O1 component

Tidal station	Observed	Computed	Difference
1. Pulau Kafai	178.5	272.4	+93.9
2 Nth Cono Island	192.4	270.0	+77.6
3 Pulau Lela	175.4	272.5	+97.1
4 Bass Harbour	183.8	224.1	+40.3
5 Penang	173.7	224.3	+50.6
6 Penang	181.9	224.3	+42.4
7. Pulau Rimau	- 160.7	253.0	+92.3
8. Lumut Pier	128.4	227.3	+98.9
9. Port Swettenham	267.6	270.0	+2.4
10. One Fathom Bank	332	273.1	-58.9
11. Pintu Gedong	288.8	270.0	-18.8
12. Pulau Undam	29.5(330.5)	294.7	-35.8
13. Muar	60.4(299.6)	293.1	-6.5
14. Kuala Batu Pahat	12.1(347.9)	294.4	-53.5
RMSE:			**63.6**

Figure 4.25: Comparison of computed and observed phases for O1 component.

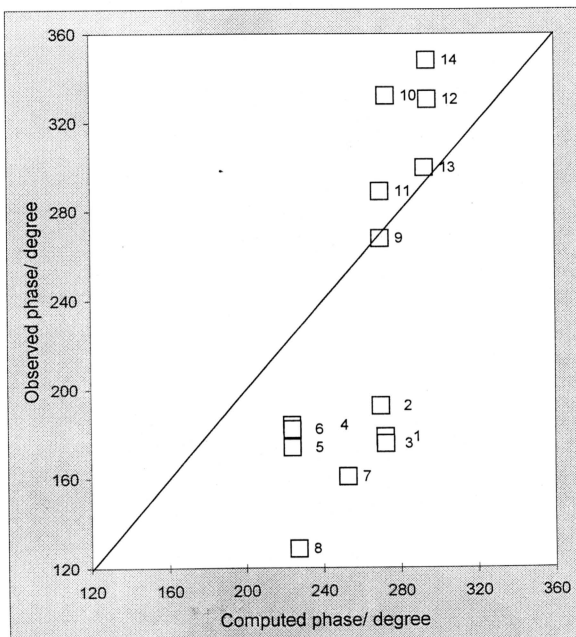

Figure 4.26: Computed co-tidal chart for O1 component in reference to Greenwich Standard Time.

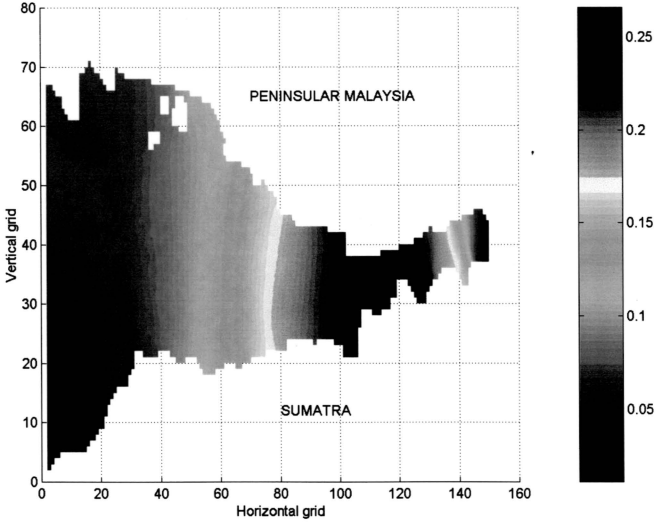

Figure 4.27: Computed co-tidal chart for O1 component in reference to Greenwich Standard Time.

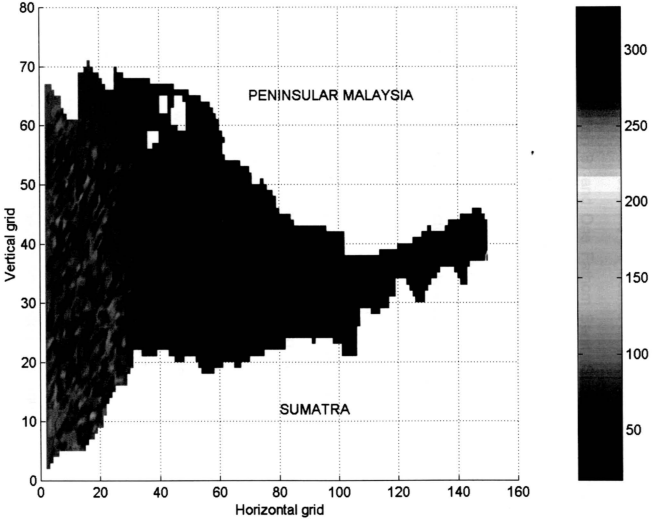

4.7.5 COMPARISON OF CURRENT SPEED AT CURRENT METER STATIONS A, B AND C

Some current data is available in the southern part of the Straits of Malacca. The better known current meter stations are located off Raleigh Shoal (Station A), Tanjung Segenting (Station B) and One Fathom Bank (Station C) as indicated previously in Figure 4.3. The data is given in terms of current amplitude for the spring and neap tides and overall tidal stream direction in Hydrographic chart No 3946 and 3947. The modelling results for M2 and S2 currents may be obtained from separate runs and combined vectorially to compute the spring (M2+S2) and neap (M2–S2) tidal constituents.

The comparisons between the computed and observed speed for spring and neap tides at these current meter stations at hourly interval for six hours before and after high water at Kuala Batu Pahat are tabulated in Tables 4.27 to 4.29 and shown plotted in Figures 4.28 to 4.33.

It may be observed that at Station A, the predicted speed of neap tide matches quite well with the published values while the spring tide is underpredicted. At Station B, the model is able to predict the speed of the neap tide very well while the speed of spring tide is again underpredicted. At Station C, the model prediction for the current speed of the spring tide is slightly lower than the published values, whereas the speed for neap tide is very much overpredicted.

Overall, the prediction of current speed has achieved satisfactory accuracy. Also, the increasing and decreasing trend of the predicted current speed seems to follow those of the published values quite closely.

Table 4.27: Comparison of computed and observed tidal current speed (spring and neap tides) at Station A (off Raleigh Shoal) referred to high water at Kuala Batu Pahat.

Time/ hours	Speed / knots (spring tides)		Speed / knots (neap tides)	
	Observed	Computed	Observed	Computed
-6	0.6	0.43	0.2	0.15
-5	0.6	0.52	0.2	0.42
-4	1.3	1.06	0.4	0.56
-3	1.5	1.21	0.4	0.59
-2	1.7	1.55	0.5	0.51
-1	1.6	1.52	0.5	0.38
0 (High water at Kuala Batu Pahat)	0.7	0.16	0.2	0.09
1	0.5	0.37	0.2	0.18
2	1	0.92	0.3	0.24
3	1.4	1.29	0.4	0.38
4	1.8	1.49	0.5	0.42
5	1.7	1.52	0.5	0.33
6	0.8	0.41	0.2	0.12

Table 4.28: Comparison of computed and observed tidal speed (spring and neap tides) at Station B (off Tanjung Segenting) referred to high water at Kuala Batu Pahat.

Time/ hours	Speed / knots (spring tides)		Speed / knots (neap tides)	
	Observed	Computed	Observed	Computed
-6	1.2	0.72	0.3	0.28
-5	0.7	0.57	0.4	0.4
-4	0	0.03	0.5	0.43
-3	0.7	0.64	0.4	0.35
-2	1.2	1.25	0.3	0.39
-1	1.5	1.03	0.1	0.02
0 (High water at Kuala Batu Pahat)	1.3	0.98	0.2	0.24
1	0.9	0.82	0.4	0.39
2	0	0.07	0.5	0.43
3	0.6	0.51	0.5	0.37
4	1.1	0.53	0.4	0.23
5	1.4	0.92	0.2	0.08
6	1.3	0.87	0.1	0.2

Table 4.29: Comparison of computed and observed tidal speed (spring and neap tides) at Station C (off One Fathom Bank) referred to high water at Kuala Batu Pahat.

Time/ hours	Speed / knots (spring tides)		Speed / knots (neap tides)	
	Observed	Computed	Observed	Computed
-6	0.8	0.93	0.3	0.42
-5	1.4	1.1	0.4	0.54
-4	1.7	1.06	0.5	0.65
-3	1.5	0.97	0.4	0.62
-2	1.1	0.86	0.3	0.43
-1	0.2	0.46	0.1	0.33
0 High water at Kuala Batu Pahat)	0.5	0.86	0.2	0.65
1	1.3	1.08	0.4	0.67
2	1.7	1.29	0.5	0.64
3	1.7	1.34	0.5	0.75
4	1.2	0.65	0.4	0.58
5	0.5	0.41	0.2	0.27
6	0.2	0.17	0.1	0.20

Figure 4.28: Comparison of computed and observed tidal current speed (spring tides) at Station A (off Raleigh Shoal) referred to high water at Kuala Batu Pahat.

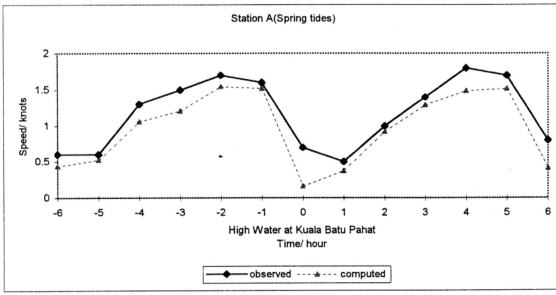

Figure 4.29: Comparison of computed and observed tidal current speed (neap tides) at Station A (off Raleigh Shoal) referred to high water at Kuala Batu Pahat.

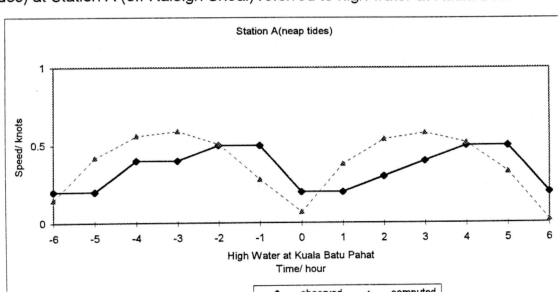

Figure 4.30: Comparison of computed and observed tidal speed (spring tides) at Station B (off Tanjung Segenting) referred to high water at Kuala Batu Pahat.

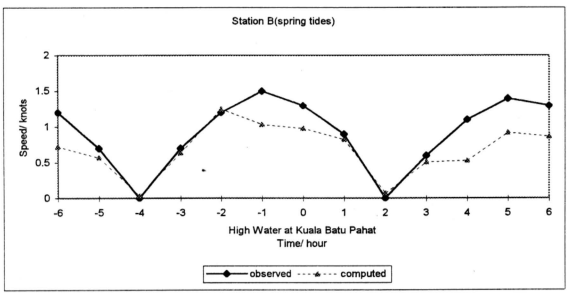

Figure 4.31: Comparison of computed and observed tidal speed (neap tides) at Station B (off Tanjung Segenting) referred to high water at Kuala Batu Pahat.

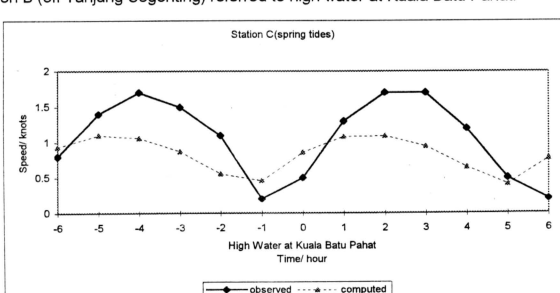

Figure 4.32: Comparison of computed and observed tidal speed (spring tides) at Station C (off One Fathom Bank) referred to high water at Kuala Batu Pahat.

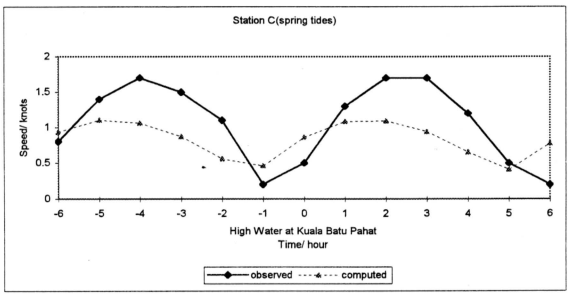

Figure 4.33: Comparison of computed and observed tidal speed (neap tides) at Station C (off One fathom Bank) referred to high water at Kuala Batu Pahat.

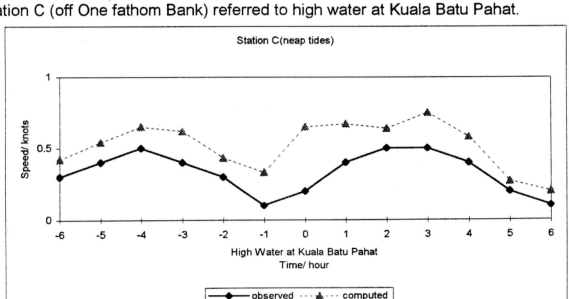

4.7.6 COMPARISON OF CURRENT DIRECTION AT CURRENT METER STATIONS A, B AND C

The modelling results for the current speed of the four components may be obtained from separate runs and combined vectorially to determine the current direction. The comparisons between the computed and observed tidal streams direction at Stations A, B and C are given in Tables 4.30 to 4.32 and shown plotted in Figures 4.34 to 4.36. The model seems to be able to predict the tidal stream direction reasonably well at Station A and B, but fares poorly against the observed values at Station C.

Table 4.30: Comparison of computed and observed tidal stream direction at Station A (off Raleigh Shoal) referred to high water at Kuala Batu Pahat.

Time/ hour	Tidal streams direction/ degree	
	Observed	Computed
-6	310	214
-5	105	129
-4	119	127
-3	127	127
-2	125	125
-1	123	124
0 (High water at Kuala Batu Pahat)	130	110
1	275	310
2	299	308
3	305	307
4	304	306
5	301	304
6	306	298

Table 4.31: Comparison of computed and observed tidal stream direction at Station B (off Tanjung Segenting) referred to high water at Kuala Batu Pahat.

Time/ hour	Tidal streams direction/ degree	
	Observed	Computed
-6	293	309
-5	290	309
-4	-	309
-3	120	294
-2	116	131
-1	115	127
0 (High water at Kuala Batu Pahat)	114	129
1	111	129
2	-	129
3	302	125
4	297	312
5	295	308
6	294	308

Table 4.32: Comparison of computed and observed tidal stream direction at Station C (off One Fathom Bank) referred to high water at Kuala Batu Pahat.

Time/ hour	Tidal streams direction/ degree	
	Observed	Computed
-6	129	88
-5	124	351
-4	121	340
-3	125	326
-2	118	315
-1	120	303
0 (High water at Kuala Batu Pahat)	312	280
1	303	204
2	304	164
3	305	149
4	305	138
5	311	127
6	129	108

Figure 4.34 Comparison of computed and observed tidal stream direction at Station A (off Raleigh Shoal) referred to high water at Kuala Batu Pahat.

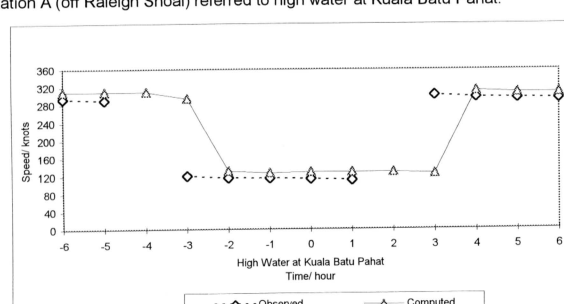

Figure 4.35 Comparison of computed and observed tidal streams direction at Station B (off Tanjung Segenting) referred to high water at Kuala Batu Pahat.

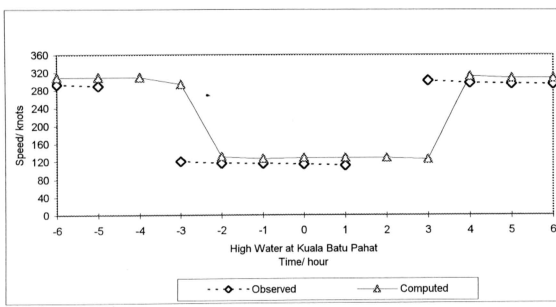

Figure 4.36 Comparison of computed and observed tidal streams direction at Station C (off One Fathom Bank) referred to high water at Kuala Batu Pahat.

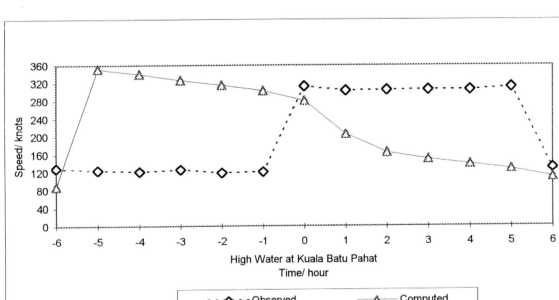

4.7.7 CURRENT DISTRIBUTION IN THE STRAITS OF MALACCA

It is generally known that the tidal current in the Straits of Malacca is in a dynamic state which oscillates in the northwest-southeast direction. However, the instantaneous snapnots of the current speed and direction could be very complex. The tidal current patterns for components M2, S2, K1 and O1 for the entire Straits are shown in Figures 4.37 to 4.40 for high water at Kuala Batu Pahat. It may be seen that generally the tidal current in the northern part is much smaller due to the large width and depth and stronger current can be seen in the narrow and shallow part of the Straits. At this time, the current in the northern portion of the Straits is towards the northwest direction whereas the direction is towards the southeast in the southern portion. On the whole, the capability of the model in producing the complex flow distribution is very encouraging.

Figure 4.37: Instantaneous velocity distribution of computed M2 component in reference to High water at Kuala Batu Pahat.

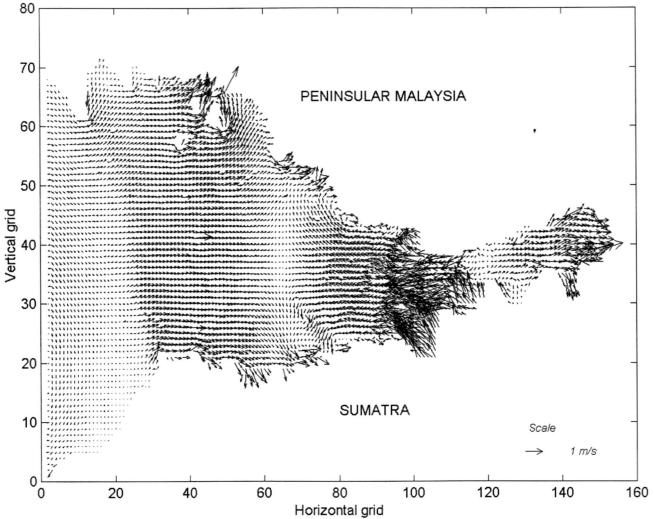

Figure 4.38: Instantaneous velocity distribution of computed S2 component in reference to High water at Kuala Batu Pahat.

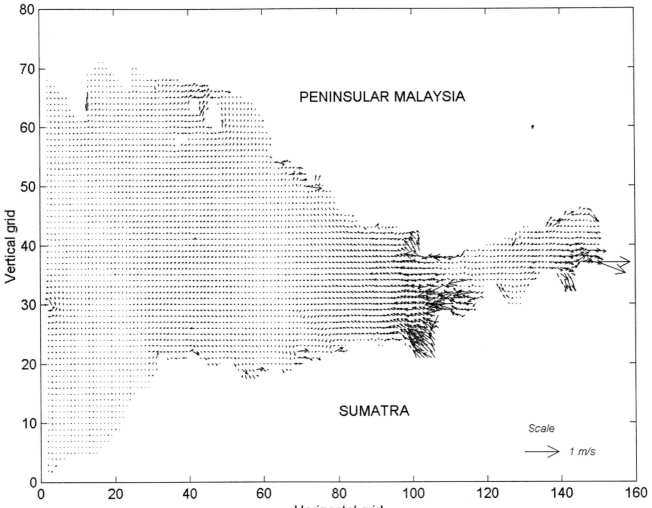

Figure 4.39: Instantaneous velocity distribution of computed K1 component in reference to High water at Kuala Batu Pahat.

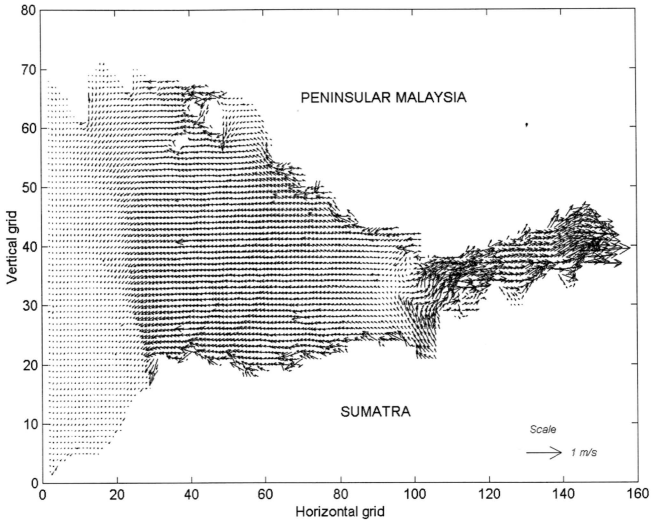

Figure 4.40: Instantaneous velocity distribution of computed O1 component in reference to High water at Kuala Batu Pahat.

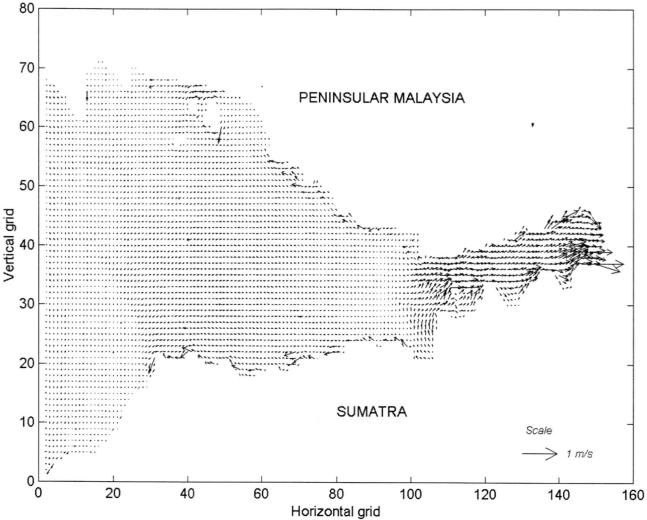

4.7.8 GENERAL DISCUSSIONS

This study represents our initial effort in formulating a two-dimensional transient tidal model for the Straits of Malacca. Overall, the results of the model show very satisfactory agreement between the computed and observed values for the main tidal constituents M2, S2, K1 and O1. The results show that the tidal features in the Straits of Malacca may be generally distinguished in two separate regions to the north and south of the constriction offshore Port Klang. Both the semidiurnal tidal components M2 and S2 exhibit maximum amplitudes in the offshore area of Port Klang due to the constriction of the Straits downstream of this region. This is consistent with the fact that the tidal energy from the Andaman Sea travelling into the Straits experiences a sudden change in depths and narrowing breadth of the Straits at this constriction and hence cause the amplitude to be hiked up. Both the diurnal components K1 and O1 show maximum amplitudes towards the southern part of the Straits. These diurnal tides originate from the South China Sea and enter the Straits from the southern opening of the Straits (Guoy, 1989).

The amplitudes of the semidiurnal tides S2 and M2 are much larger than those of the diurnal tides K1 and O1 in the northern of the Straits whereas they are almost of the same amplitude in the southern part of the Straits. This suggests that the effects of semidiurnal tides are more apparent in the north while the contributions of the diurnal tides are equally significant as the semidiurnal tides in the south. Therefore, it can be concluded that the semidiurnal tides are the main

sources that dominate the northern tidal flow pattern whereas the southern part of the Straits contains a mixture of semidiurnal and diurnal components.

The accuracy of the predictions depends very much on the correct representation of all the real features of the Straits of Malacca in the model and the reliability of the input data. In the model, the inundated coastlines and the abrupt changes in at many places may not have been well represented within a single cell. This will certainly affect the accuracy of the results especially for tidal stations that are very close to the coast. A better representation of the coastline by using smaller grids at appropriate places is required in order to reproduce the detail information for more accurate prediction. In view of the paucity of reliable input data for water depth, bottom friction coefficient and tidal elevations in open boundaries, the use of data assimilation technique may help to improve the prediction.

There has recently been considerable interest in the data assimilation techniques by incorporating measured data into the numerical model. In recent years, systematic techniques based on optimal control methods have been developed, particularly in the field of meteorology. Much of the review on such techniques can be found in Lorenc,1986, Navon,1986 and Le Dimet and Navon, 1989, Zou, et al. 1992. In the field of oceanography, such methods have also come into use for tidal flow problem. Smedstad, 1989, and Smedstad and O'Brien, 1991 have used this approach to determine the effective phase speed in a model of the equatorial Pacific Ocean based on observations of sea level. Yu and O'Brien, 1991 have used a similar method to estimate the eddy viscosity and surface drag

coefficient from measured velocities of a wind-driven flow. Das and Larner, 1991 have estimated the position dependent drag and depth in a sectionally integrated model of flow in a channel by assimilating periodic tidal data and compared several minimization algorithms. Lardner, 1993 has used similar variational techniques to estimate the open boundary conditions in a two-dimensional tidal model. Das and Lardner, 1992, have extended their earlier work to the estimation of the parameters for the same two-dimensional model.

The variational method involves minimizing a certain cost function which consists of the norm of the differences between the computed and observed values of the measured variables such as the surface elevations at tidal gauges. The given boundary value problem dictated by the tidal governing equations forms a constraint on the minimization. Construction of the gradient of the cost function with respect to various unknown parameters leads to an adjoint problem that could be solved backward in time using the numerical optimization algorithms. It is known that a major difficulty with applications of the adjoint method is the very large demand on computer memory (Lardner, et al, 1993).